PHYSICAL REVIEW C **82**, 045210 (2010)

$\bar{K}^*$ mesons in dense matter

L. Tolós,[1,*] R. Molina,[2] E. Oset,[2] and A. Ramos[3]

[1]*Theory Group KVI, University of Groningen, Zernikelaan 25, NL-9747 AA Groningen, The Netherlands*

[2]*Instituto de Física Corpuscular (Centro Mixto CSIC-UV), Institutos de Investigación de Paterna, Apartado 22085, ES-46071 Valencia, Spain*

[3]*Departament d'Estructura i Constituents de la Matèria i Institut de Ciències del Cosmos. Facultat de Física. Universitat de Barcelona, Avda. Diagonal 647, 08028 Barcelona, Spain*

(Received 17 June 2010; revised manuscript received 10 September 2010; published 29 October 2010)

We study the properties of $\bar{K}^*$ mesons in nuclear matter using a unitary approach in coupled channels within the framework of the local hidden gauge formalism and incorporating the $\bar{K}\pi$ decay channel in matter. The in-medium $\bar{K}^*N$ interaction accounts for Pauli blocking effects and incorporates the $\bar{K}^*$ self-energy in a self-consistent manner. We also obtain the $\bar{K}^*$ (off-shell) spectral function and analyze its behavior at finite density and momentum. At a normal nuclear matter density, the $\bar{K}^*$ meson feels a moderately attractive potential, while the $\bar{K}^*$ width becomes five times larger than in free space. We estimate the transparency ratio of the $\gamma A \to K^+ K^{*-} A'$ reaction, which we propose as a feasible scenario at the present facilities to detect changes in the properties of the $\bar{K}^*$ meson in nuclear medium.

DOI: 10.1103/PhysRevC.82.045210 PACS number(s): 14.20.Gk, 11.10.St, 13.75.Jz, 21.65.−f

I. INTRODUCTION

The interaction of vector mesons with nuclear matter has been the focus of attention for years and has been tied to fundamental aspects of QCD [1–3]. Yet the theoretical models offer a large variety of results for a large attraction to a large repulsion. Early results on this issue within the Nambu Jona Lasinio model produced no shift of the masses [4], while using qualitative arguments, a universal large attractive shift of the mass was suggested in Ref. [5]. More recent detailed calculations show no shift of the mass of the ρ meson in matter [6–10] and a very small shift for the ϕ meson [11]. Experimentally the situation has undergone big strides recently, an example being the NA60 Collaboration, which reported a null shift of the ρ mass in the medium [12–14] in the dilepton spectra of heavy-ion reactions. Detailed theoretical analyses of the reaction were also done in Refs. [15] and [16], confirming those conclusions and leaving room for some widening of the resonance. Similarly, a null shift in the γ-induced dilepton production at CLAS was also found in Refs. [17] and [18]. In contrast, the KEK team had earlier reported an attractive mass shift of the ρ in [19] and [20]. As explained in detail in Ref. [17], the different conclusions can be traced back to the way the background is subtracted.

The case of the ω in the medium has been more controversial. Theoretically, there are about 20 works claiming a variety of mass shifts, from largely attractive to largely repulsive (see Refs. [21–26] for details). Experimentally, a large shift of the mass of the ω was reported in a study of photon-induced ω production in nuclei, with the ω being detected through its $\pi^0\gamma$ decay channel [27]. However, it was shown in Ref. [25] that the shift could just be the consequence of a particular choice of background subtraction and that other reasonable choices led to different conclusions. In fact, a recent reanalysis of the background of the reaction concluded that one cannot determine the shift of the ω mass in the nucleus from that reaction [28]. In contrast, determination of the ω width in the medium by means of the production cross section in different nuclei, which leads to the transparency ratio [29], was rather successful, giving rise to an appreciable in-medium enhancement [25,30].

Curiously, there has been no discussion about the properties of the strange vector mesons in the medium, and this is the purpose of the present paper. The reason might be that not much attention has been paid to the interaction of K^* and $\bar{K}^*$ mesons with baryons. The fact that the $\bar{K}^*$ cannot be detected with dileptons might also be a reason for the experimental neglect. The situation was reversed only recently in Ref. [31], based on the assumption that the interaction between light quarks is spin independent and SU(3) flavor independent, and in Refs. [32] and [33], where this problem was tackled using the hidden local gauge formalism for the interaction of vector mesons with baryons of the octet and the decuplet. The study in Ref. [33] allows us to obtain the $\bar{K}^*$ self-energy in the nuclear medium, following an approach similar to the one employed in Ref. [34] for the interaction of $\bar{K}$ in the medium starting from the $\bar{K}N$ interaction using the chiral unitary approach [35]. We find that, while the $\bar{K}^*$ shows a moderately attractive optical potential at normal nuclear matter density, there is a spectacular enhancement of the $\bar{K}^*$ width in the medium, up to about 5 times the free value of about 50 MeV. We also perform a qualitative estimate of the transparency ratio for $\bar{K}^*$ production in the $\gamma A \to K^+ \bar{K}^{*-} A'$ reaction, to motivate experimental study of this remarkable medium property.

The paper is organized as follows: the formalism is presented in Sects. II and III, where we first review how the $\bar{K}^*N$ interaction in the free space is obtained and, next, describe the calculation of the $\bar{K}^*$ self-energy in nuclear matter, with contributions coming from the $\bar{K}^*N$ absorption mechanism as well as from $\bar{K}^*$ decay into $\bar{K}\pi$ in dense matter. In Sec. IV we show the results obtained for the $\bar{K}^*$ properties in the medium, while in Sec. V we provide an overview of the method including a critical discussion and

*tolos@kvi.nl

future developments. Section VI presents the corresponding nuclear transparency ratio in the $\gamma A \to K^* K^{*-} A'$ reaction, and our conclusions and outlook are given in Sec. VII.

II. $\bar{K}^* N$ INTERACTION IN FREE SPACE

In this section we present a review of the formalism used for building up the interaction of vector mesons with baryons in free space. Medium modifications are incorporated in the next section to obtain the $\bar{K}^*$ self-energy in nuclear matter.

To construct the interaction of vector mesons with baryons, we first obtain the interaction between vector mesons. We follow the formalism of the hidden gauge interaction for vector mesons in Refs. [36–39] (see also Ref. [40] for a practical set of Feynman rules). The Lagrangian involving interactions among vector mesons is given by

$$\mathcal{L}_{III} = -\tfrac{1}{4}\langle V_{\mu\nu} V^{\mu\nu}\rangle, \tag{1}$$

where the symbol $\langle\rangle$ stands for the trace in the SU(3) space and $V_{\mu\nu}$ is given by

$$V_{\mu\nu} = \partial_\mu V_\nu - \partial_\nu V_\mu - ig[V_\mu, V_\nu], \tag{2}$$

where g is

$$g = \frac{M_V}{2f}, \tag{3}$$

with M_V being the vector meson mass and $f = 93$ MeV the pion decay constant. The value of g given by the relation in Eq. (3) fulfills the KSFR rule [41], which is tied to vector meson dominance [42]. The magnitude V_μ is the SU(3) matrix of the vectors of the octet of the ρ plus the SU(3) singlet:

$$V_\mu = \begin{pmatrix} \frac{\rho^0}{\sqrt{2}} + \frac{\omega}{\sqrt{2}} & \rho^+ & K^{*+} \\ \rho^- & -\frac{\rho^0}{\sqrt{2}} + \frac{\omega}{\sqrt{2}} & K^{*0} \\ K^{*-} & \bar{K}^{*0} & \phi \end{pmatrix}_\mu . \tag{4}$$

From this Lagrangian we obtain a three-vector vertex term,

$$\mathcal{L}_{\rm III}^{(3V)} = ig\langle (V^\mu \partial_\nu V_\mu - \partial_\nu V_\mu V^\mu) V^\nu\rangle, \tag{5}$$

analogous to the coupling of vectors to pseudoscalars. In a similar way, one obtains the Lagrangian for the coupling of vector mesons to the baryon octet, given by [43,44]

$$\mathcal{L}_{BBV} = g(\langle \bar{B}\gamma_\mu [V^\mu, B]\rangle + \langle \bar{B}\gamma_\mu B\rangle\langle V^\mu\rangle), \tag{6}$$

where B is now the SU(3) matrix of the baryon octet,

$$B = \begin{pmatrix} \frac{1}{\sqrt{2}}\Sigma^0 + \frac{1}{\sqrt{6}}\Lambda & \Sigma^+ & p \\ \Sigma^- & -\frac{1}{\sqrt{2}}\Sigma^0 + \frac{1}{\sqrt{6}}\Lambda & n \\ \Xi^- & \Xi^0 & -\frac{2}{\sqrt{6}}\Lambda \end{pmatrix}. \tag{7}$$

With these ingredients we can construct the Feynman diagrams that lead to the vector-baryon (VB) transitions $VB \to V'B'$. As discussed in Ref. [33], one can proceed by neglecting the three-momentum of the external vectors versus the vector mass, in a similar way as done for chiral Lagrangians under the low-energy approximation, and one obtains the transition potential,

$$V_{ij} = -C_{ij}\frac{1}{4f^2}(k^0 + k'^0)\vec{\epsilon}\vec{\epsilon}', \tag{8}$$

where k^0 and k'^0 are the energies of the incoming and outgoing vector mesons, respectively, $\vec{\epsilon}\vec{\epsilon}'$ is the product of their polarization vectors, and C_{ij} are the symmetry coefficients [33].

The meson-baryon scattering amplitude is obtained from the coupled-channel on-shell Bethe-Salpeter equation [35,45],

$$T = [1 - VG]^{-1} V, \tag{9}$$

with G being the loop function of a vector meson of mass m and a baryon of mass M with total four-momentum P ($s = P^2$):

$$G(s, m^2, M^2) = i2M \int \frac{d^4q}{(2\pi)^4} \frac{1}{(P-q)^2 - M^2 + i\epsilon} \frac{1}{q^2 - m^2 + i\epsilon}, \tag{10}$$

which is conveniently regularized [45], taking a natural value of -2 for the subtraction constants at a regularization scale $\mu = 630$ MeV [33].

We note that the iteration of diagrams implicit in the Bethe-Salpeter equation for vector-meson scattering implies a sum over the polarizations of the internal vector mesons, which, because they are tied to the external ones through the $\vec{\epsilon}\vec{\epsilon}'$ factor, leads to a correction in the G function of $\vec{q}^2/3M_V^2$ [46], a factor that can be safely neglected in consonance with the low-momentum approximation done. This leads to factorization of the factor $\vec{\epsilon}\vec{\epsilon}'$ for external vector mesons also in the T matrix. This method provides degenerate pairs of resonances that have $J^P = 1/2^-, 3/2^-$, a pattern that seems to be reproduced by the existing experimental data [see, in the Particle Data Group (PDG) study [47], states $N^*(1650)(1/2^-)$, $N^*(1700)(3/2^-)$, $N^*(2080)(3/2^-)$, $N^*(2090)(1/2^-)$, $\Sigma(1940)(3/2^-)$, $\Sigma(2000)(1/2^-)$, $\Delta(1900)(1/2^-)$, $\Delta(1940)(3/2^-)$, and $\Delta(1930)(5/2^-)$].

Because we are interested in studying the interaction of $\bar{K}^*$ mesons in nuclear matter, we concentrate on the strangeness $S = -1$ vector meson-baryon sector with isospin $I = 0$ and $I = 1$. For $S = -1$, $I = 0$, we find five vector meson-baryon coupled channels ($\bar{K}^* N$, $\omega\Lambda$, $\rho\Sigma$, $\phi\Lambda$, and $K^*\Xi$), while for $S = -1$, $I = 1$, we consider six channels ($\bar{K}^* N$, $\rho\Lambda$, $\rho\Sigma$, $\omega\Sigma$, $K^*\Xi$, and $\phi\Sigma$).

The relatively large decay width of the ρ and $\bar{K}^*$ vector mesons (into $\pi\pi$ or $\bar{K}\pi$ pairs, respectively) is incorporated in the loop functions via the convolution [48]

$$\tilde{G}(s) = \frac{1}{N}\int_{(m-\Delta_l)^2}^{(m+\Delta_r)^2} d\tilde{m}^2 \left(-\frac{1}{\pi}\right) \times \mathrm{Im}\frac{1}{\tilde{m}^2 - m^2 + i m\Gamma(\tilde{m})} G(s, \tilde{m}^2, M^2), \tag{11}$$

with

$$N = \int_{(m-\Delta_l)^2}^{(m+\Delta_r)^2} d\tilde{m}^2 \left(-\frac{1}{\pi}\right) \mathrm{Im}\frac{1}{\tilde{m}^2 - m^2 + i m\Gamma(\tilde{m})} \tag{12}$$

being the normalization factor. The integration range around the meson mass is established by the left and right parameters Δ_l and Δ_r, taken to be a few times the meson width Γ, the value of which is 149.4 MeV for the ρ meson and 50.5 MeV for

the $\bar{K}^*$ meson. The energy-dependent width $\Gamma(\tilde{m})$ is obtained from

$$\Gamma(\tilde{m}) = \Gamma \frac{m^2}{\tilde{m}^2} \frac{q(\tilde{m})^3}{q(m)^3} \theta(\tilde{m} - m_1 - m_2), \tag{13}$$

where $q(\sqrt{s})$ is the momentum of the decay products in the rest frame of the vector meson with invariant mass $\sqrt{s}$. In the case of ρ decay we have $m_1 = m_2 = m_\pi$, while for $\bar{K}^*$ decay, $m_1 = m_\pi$, $m_2 = m_{\bar{K}}$.

III. $\bar{K}^*$ SELF-ENERGY IN NUCLEAR MATTER

There are two sources for the modification of $\bar{K}^*$ self-energy in nuclear matter: (a) the contribution associated with the decay mode $\bar{K}\pi$ modified by the nuclear medium effects on the $\bar{K}$ and π mesons and (b) the contribution associated with the interaction of the $\bar{K}^*$ with the nucleons in the medium, which accounts for the direct quasielastic process $\bar{K}^* N \to \bar{K}^* N$ as well as other absorption channels, $\bar{K}^* N \to \rho Y, \omega Y, \phi Y, \ldots$, with $Y = \Lambda, \Sigma$.

A. $\bar{K}^*$ self-energy from decay into $\bar{K}\pi$

We devote this section to study of the decay of the $\bar{K}^*$ meson into $\bar{K}\pi$ pairs renormalized in the medium. First, to test our model, we evaluate the theoretical width in the vacuum, indicated by the diagram on the left in Fig. 1, including the $K^{*-} \to \bar{K}^0 \pi^-$ and $K^{*-} \to \bar{K}^- \pi^0$ processes, which gives

$$\Pi^0_{\bar{K}^*}(q^0, \vec{q}) = 2g^2 \vec{\epsilon} \cdot \vec{\epsilon}' \int \frac{d^4k}{(2\pi)^4} \frac{\vec{k}^2}{k^2 - m_\pi^2} \frac{1}{(q-k)^2 - m_{\bar{K}}^2 + i\epsilon}, \tag{14}$$

where the VPP vertices were obtained from the hidden gauge Lagrangian of $\mathcal{L}_{VPP} = -ig\langle V^\mu [\phi, \partial_\mu \phi]\rangle$ [36,40], within the low-momentum approximation employed in the present work. This approximation has allowed us to keep only the spatial components of the vector polarizations, which means substituting $\epsilon_\mu k^\mu \epsilon'_\nu k^\nu$ with $\epsilon_i k_i \epsilon'_j k_j$, a factor that was further replaced in the integral by $\vec{\epsilon} \cdot \vec{\epsilon}' \frac{1}{3} \vec{k}^2 \delta_{ij}$.

The imaginary part of the free $\bar{K}^*$ self-energy at rest,

$$\mathrm{Im}\Pi^0_{\bar{K}^*}(q^0 = m_{\bar{K}^*}, \vec{q} = 0) = \frac{g^2}{4\pi} \vec{\epsilon} \cdot \vec{\epsilon}' |\vec{k}|^3 \frac{1}{m_{\bar{K}^*}}, \tag{15}$$

where the momentum of the emitted mesons is $|\vec{k}| = 288.7$ MeV, determines a value of the K^{*-} width of $\Gamma_{K^{*-}} = -\mathrm{Im}\Pi^0_{\bar{K}^*}/m_{\bar{K}^*} = 42$ MeV, which is quite close to the experimental value $\Gamma^{\mathrm{exp}}_{K^{*-}} = 50.8 \pm 0.9$ MeV.

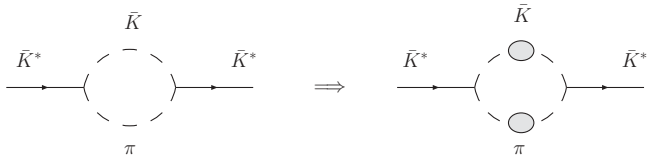

FIG. 1. The $\bar{K}$ propagator renormalized to allow its decay into $\bar{K}\pi$, in the free space (left) and in the medium (right), including the self-energies of the $\bar{K}$ and π mesons.

In the medium we calculate the $\bar{K}^*$ self-energy coming from its decay into $\bar{K}\pi$ including the self-energy of both the antikaon and the pion. This will add new contributions to the $\bar{K}^*$ self-energy such as the one depicted by the diagram on the right in Fig. 1.

For completeness, we briefly recall the essential features of the models employed for the properties of antikaons and pions in nuclear matter. We refer to Refs. [34] and [49–54] for a detailed explanation.

The $\bar{K}$ self-energy in symmetric nuclear matter is obtained from the antikaon-nucleon interaction within a chiral unitary approach. The model incorporates s and p waves in the interaction and includes the following channels: $\bar{K}N$, $\pi\Sigma$, $\eta\Lambda$, and $K\Xi$ for $I = 0$, and $\bar{K}N$, $\pi\Lambda$, $\pi\Sigma$, $\eta\Sigma$, and $K\Xi$ for $I = 1$. The tree-level s-wave amplitudes are given by the Weinberg-Tomozawa term of the lowest order chiral Lagrangian describing the interaction of the pseudoscalar meson octet with the $1/2^+$ baryon octet. Unitarization in coupled channels is imposed by solving the Bethe-Salpeter equation with on-shell amplitudes. Loops incorporate in-medium effects, which include Pauli blocking corrections, as well as mean-field binding on the nucleons and hyperons via a σ-ω model. They are regularized with a cutoff momentum of $q_{\mathrm{max}} = 630$ MeV. Self-consistency in the $\bar{K}$ self-energy is also required. The p-wave contribution to the $\bar{K}$ self-energy is built up from the coupling of the $\bar{K}$ meson to ΛN^{-1}, ΣN^{-1}, and $\Sigma^* N^{-1}$ excitations.

The model determines an attractive optical potential of $U_{K^-} = \mathrm{Re}\Pi_{K^-}/2m_{K^-} \sim -66$ MeV. This attraction is quite moderate in comparison with that in other approximation schemes [56,57,59–62], although it agrees with others that also implement self-consistency [63–67].

The pion self-energy consists of a small s-wave part, $\Pi^{(s)}_\pi(\rho)$ (momentum independent), and a dominant p-wave component, $\Pi^{(p)}_\pi(k^0, \vec{k}, \rho)$, which comes from particle-hole (NN^{-1} or ph) and ΔN^{-1} excitations [50]. The model also includes a two-particle/two-hole (2p2h) piece tied to two-nucleon pion absorption. The strength of the considered collective modes is modified by repulsive, spin-isospin NN and $N\Delta$ short-range correlations, which are included in a phenomenological way with a single Landau-Migdal interaction parameter, g' [51].

Replacing the pion and antikaon propagators in Eq. (14) with their respective propagators in the medium, written in the Lehmann representation, gives

$$\begin{aligned} -i\Pi^{\rho,(a)}_{\bar{K}^*}(q^0, \vec{q}) &= 2g^2 \vec{\epsilon} \cdot \vec{\epsilon}' \int \frac{d^4k}{(2\pi)^4} \vec{k}^2 \int_0^\infty \frac{d\omega}{\pi} (-2\omega) \frac{\mathrm{Im}D_\pi(\omega, \vec{k})}{(k^0)^2 - \omega^2 + i\epsilon} \\ &\times \int_0^\infty \frac{d\omega'}{\pi} (-) \left\{ \frac{\mathrm{Im}D_{\bar{K}}(\omega', \vec{q} - \vec{k})}{q^0 - k^0 - \omega' + i\eta} \right. \\ &\left. - \frac{\mathrm{Im}D_K(\omega', \vec{q} - \vec{k})}{q^0 - k^0 + \omega' - i\eta} \right\}, \end{aligned} \tag{16}$$

which, after integrating over the k^0 variable, becomes

$$\Pi^{\rho,(a)}_{\bar{K}^*}(q^0,\vec{q}) = 2g^2\vec{\epsilon}\cdot\vec{\epsilon}'\int\frac{d^3k}{(2\pi)^3}\frac{\vec{k}^2}{\pi^2}\int_0^\infty d\omega\,\mathrm{Im}D_\pi(\omega,\vec{k}) \times\int_0^\infty d\omega'\left\{\frac{\mathrm{Im}D_{\bar{K}}(\omega',\vec{q}-\vec{k})}{q^0-\omega-\omega'+i\eta} - \frac{\mathrm{Im}D_K(\omega',\vec{q}-\vec{k})}{q^0+\omega+\omega'-i\eta}\right\}. \quad (17)$$

Because we are using the physical mass of the $\bar{K}^*$, the real part of this in-medium self-energy must vanish at $\rho=0$. This is achieved by subtracting the real part of the free $\bar{K}^*$ self-energy, $\Pi^0_{\bar{K}^*}$, from $\Pi^{\rho,(a)}_{\bar{K}^*}$. The part of the negative energy of the $\bar{K}$ propagator represented by the last term in Eq. (17) is small; it does not contribute to the imaginary part of the $\bar{K}^*$ self-energy; and, to a very good approximation, it can be canceled by the corresponding term of the free $\bar{K}^*$ self-energy. Hence, we can write the $\bar{K}^*$ self-energy as

$$\Pi^{\rho,(a)}_{\bar{K}^*}(q^0,\vec{q}) = 2g^2\vec{\epsilon}\cdot\vec{\epsilon}'\left\{\int\frac{d^3k}{(2\pi)^3}\frac{\vec{k}^2}{\pi^2}\int_0^\infty d\omega\,\mathrm{Im}D_\pi(\omega,\vec{k}) \times\int_0^\infty d\omega'\frac{\mathrm{Im}D_{\bar{K}}(\omega',\vec{q}-\vec{k})}{q^0-\omega-\omega'+i\eta} - \mathrm{Re}\int\frac{d^3k}{(2\pi)^3}\frac{\vec{k}^2}{2\omega_\pi(k)}\frac{1}{2\omega_{\bar{K}}(q-k)} \times\frac{1}{q^0-\omega_\pi(k)-\omega_{\bar{K}}(q-k)+i\epsilon}\right\}. \quad (18)$$

One still has to implement vertex corrections that are required by the gauge invariance of the model [68,69] and are associated with the last three diagrams in Fig. 2. As shown in Sec. IV, the effect of dressing the pion is considerably larger than that of including the $\bar{K}$ self-energy. Therefore, we consider the vertex corrections only for the case of the pion. They can be easily implemented by evaluating the first diagram in Fig. 2 but replacing the p-wave pion self-energy with

$$\Pi^{(p)}_\pi \Longrightarrow \frac{\Pi^{(p)}_\pi}{\vec{k}^2}\left(\vec{k}^2+\left[D^0_\pi(k)\right]^{-1}+\frac{3}{4}\frac{\left[D^0_\pi(k)\right]^{-2}}{\vec{k}^2}\right), \quad (19)$$

where $[D^0_\pi(k)]^{-1}=(k^0)^2-\vec{k}^2-m_\pi^2$ [55].

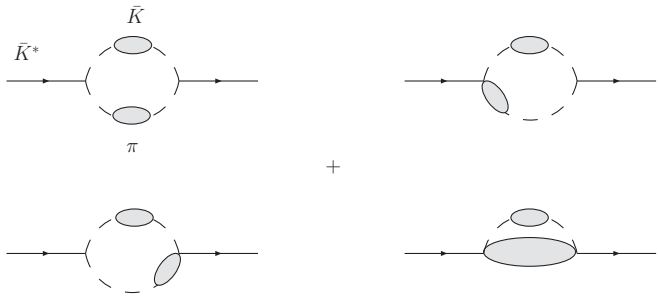

FIG. 2. Self-energy diagrams at first order in the nuclear density contributing to the decay of the $\bar{K}^*$ meson in the medium.

B. $\bar{K}^*$ self-energy from the s-wave $\bar{K}^*N$ interaction

In this section we consider the contributions to the $\bar{K}^*$ self-energy coming from its interactions with nucleons in the Fermi sea. These are implemented by incorporating the corresponding medium modifications in the effective $\bar{K}^*N$ interaction. One of the sources of density dependence comes from the Pauli principle acting on the nucleons, which prevents them from being scattered into already occupied states. Another source is related to the change in the properties of mesons and baryons in the coupled-channel states owing to the interaction with nucleons in the Fermi sea. In particular, we consider the self-consistently calculated $\bar{K}^*$ self-energy in the $\bar{K}^*N$ intermediate states.

We proceed as done in Ref. [58]. Formally, the meson-baryon propagator in nuclear matter reads

$$G^\rho(P) = G^0(\sqrt{s}) + \lim_{\Lambda\to\infty}\delta G^\rho_\Lambda(P),$$
$$\delta G^\rho_\Lambda(P) \equiv G^\rho_\Lambda(P) - G^0_\Lambda(\sqrt{s}) = \mathrm{i}2M\int_\Lambda\frac{d^4q}{(2\pi)^4} \times\left(D^\rho_{\mathcal{B}}(P-q)D^\rho_{\mathcal{M}}(q) - D^0_{\mathcal{B}}(P-q)D^0_{\mathcal{M}}(q)\right), \quad (20)$$

where $\sqrt{s}$ is the center-of-mass energy and q and $P-q$ are the meson and baryon four-momentum, respectively. The meson-baryon loop G^0 is calculated using dimensional regularization, while the medium $\delta G^\rho = \lim_{\Lambda\to\infty}\delta G^\rho_\Lambda(P)$ correction contains all the nuclear medium effects affecting the loop. This quantity is calculated in the infinite cutoff limit, and therefore, it is UV finite and independent of the selected subtracting point used to regularize G^0.

For the $\bar{K}^*N$ channel we consider Pauli blocking effects on the nucleons together with self-energy insertions of the $\bar{K}^*$ meson. The self-energy is obtained self-consistently from the in-medium $\bar{K}^*N$ effective interaction, $T^\rho{}_{\bar{K}^*N}$, as we show in the following. The corresponding in-medium single-particle propagators are then given by

$$D^\rho_N(p) = \frac{1}{2E_N(\vec{p})}\left\{\sum_r u_r(\vec{p})\bar{u}_r(\vec{p})\left(\frac{1-n(\vec{p})}{p^0-E_N(\vec{p})+i\varepsilon} + \frac{n(\vec{p})}{p^0-E_N(\vec{p})-i\varepsilon}\right) + \frac{\sum_r v_r(-\vec{p})\bar{v}_r(-\vec{p})}{p^0+E_N(\vec{p})-i\varepsilon}\right\} = D^0_N(p) + 2\pi i n(\vec{p})\frac{\delta(p^0-E_N(\vec{p}))}{2E_N(\vec{p})}\sum_r u_r(\vec{p})\bar{u}_r(\vec{p}), \quad (21)$$

$$D^\rho_{\bar{K}^*}(q) = ((q^0)^2-\omega(\vec{q})^2-\Pi_{\bar{K}^*}(q))^{-1} = \int_0^\infty d\omega\left(\frac{S_{\bar{K}^*}(\omega,\vec{q})}{q^0-\omega+i\varepsilon} - \frac{S_{K^*}(\omega,\vec{q})}{q^0+\omega-i\varepsilon}\right), \quad (22)$$

where $E_N(\vec{p})=\sqrt{\vec{p}^2+M_N^2}$ and $\omega(\vec{q})=\sqrt{\vec{q}^2+m^2_{\bar{K}^*}}$ are the nucleon and $\bar{K}^*$ energies, respectively, $\Pi_{\bar{K}^*}(q^0,\vec{q})$ is the $\bar{K}^*$ meson self-energy, and $S_{\bar{K}^*}$ is the corresponding meson

spectral function. In a very good approximation the spectral function for the K^* meson can be approximated by the free-space one, that is, by a δ function, because there are no baryon resonances in the strangeness $S = 1$ case. Finally, $n(\vec{p})$ is the Fermi gas nucleon momentum distribution, given by the step function $n(\vec{p}) = \Theta(p_F - |\vec{p}|)$, with $p_F = (3\pi^2\rho/2)^{1/3}$.

Using Eq. (20) and performing the energy integral over q^0, the $\bar{K}^*N$ loop function reads

$$G^{\rho}{}_{\bar{K}^*N}(P) = G^0_{\bar{K}^*N}(\sqrt{s}) + \int \frac{d^3q}{(2\pi)^3}\frac{M_N}{E_N(\vec{p})} \times \left[\frac{-n(\vec{p})}{[P^0 - E_N(\vec{p})]^2 - \omega(\vec{q})^2 + i\varepsilon} + [1 - n(\vec{p})]\left(\frac{-1/[2\omega(\vec{q})]}{P^0 - E_N(\vec{p}) - \omega(\vec{q}) + i\varepsilon} + \int_0^\infty d\omega \frac{S_{\bar{K}^*}(\omega, \vec{q})}{P^0 - E_N(\vec{p}) - \omega + i\varepsilon}\right)\right]\Bigg|_{\vec{p}=\vec{P}-\vec{q}}, \tag{23}$$

where the first term of the integral, proportional to $-n(\vec{p})$, is the Pauli correction and accounts for the case where the Pauli blocking on the nucleon is considered and the meson in-medium self-energy is neglected. The second term, proportional to $[1 - n(\vec{p})]$, would be exactly 0 if the meson spectral function $S_{\bar{K}^*}$ was the free one, $S^0_{\bar{K}^*}(\omega, \vec{q}) = \delta[\omega - \omega(\vec{q})]/(2\omega)$. Then it accounts for the contribution of the in-medium meson modification to the loop function.

For all other meson-baryon states we use the free loop functions given by Eq. (10) [or Eq. (11) for ρ-baryon states] because these meson-baryon states couple more moderately to the $\bar{K}^*N$ channel.

We can now solve the on-shell Bethe-Salpeter equation in nuclear matter for the in-medium amplitudes in the isospin basis:

$$T^{\rho(I)}(P) = \frac{1}{1 - V^I(\sqrt{s})G^{\rho(I)}(P)}V^I(\sqrt{s}). \tag{24}$$

The in-medium $\bar{K}^*$ self-energy is then obtained by integrating $T^{\rho}{}_{\bar{K}^*N}$ over the nucleon Fermi sea,

$$\Pi^{\rho,(\mathrm{b})}_{\bar{K}^*}(q^0, \vec{q}) = \int \frac{d^3p}{(2\pi)^3} n(\vec{p})\left[T^{\rho(I=0)}_{\bar{K}^*N}(P^0, \vec{P}) + 3T^{\rho(I=1)}_{\bar{K}^*N}(P^0, \vec{P})\right], \tag{25}$$

where $P^0 = q^0 + E_N(\vec{p})$ and $\vec{P} = \vec{q} + \vec{p}$ are the total energy and momentum of the $\bar{K}^*N$ pair in the nuclear-matter rest frame, and the values $(q^0, \vec{q})$ stand for the energy and momentum of the $\bar{K}^*$ meson also in this frame. The self-energy $\Pi^{\rho,(\mathrm{b})}_{\bar{K}^*}(q^0, \vec{q})$ has to be determined self-consistently, as it is obtained from the in-medium amplitude $T^{\rho}_{\bar{K}^*N}$, which contains the $\bar{K}^*N$ loop function $G^{\rho}_{\bar{K}^*N}$, and the latter quantity itself is a function of $\Pi^{\rho}_{\bar{K}^*} = \Pi^{\rho,(\mathrm{a})}_{\bar{K}^*} + \Pi^{\rho,(\mathrm{b})}_{\bar{K}^*}$. From this self-energy we obtain the corresponding spectral function, which is used in the integral for the loop function $G^{\rho}{}_{\bar{K}^*N}(P^0, \vec{P})$, as given in Eq. (23).

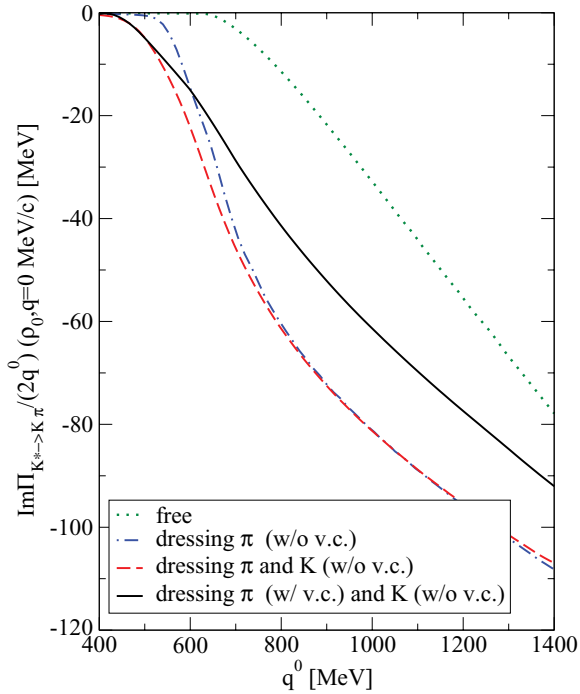

FIG. 3. (Color online) Imaginary part of the $\bar{K}^*$ self-energy at zero momentum, coming from the $\bar{K}\pi$ decay mode in dense matter at normal saturation density ρ_0. Different approaches are studied: (i) calculation in free space, (ii) including the π self-energy, (iii) including the π and $\bar{K}$ self-energies, and (iv) including the π dressing with vertex corrections and the $\bar{K}$ self-energy.

IV. RESULTS

In Fig. 3 we show the energy dependence of the imaginary part of the $\bar{K}^*$ self-energy for $\vec{q} = 0$ coming from $\bar{K}\pi$ decay, in free space (dotted line), adding the π self-energy (dot-dashed line) at normal nuclear matter saturation density ($\rho_0 = 0.17$ fm^{-3}), and including both the π and the $\bar{K}$ self-energy contributions (dashed line). Figure 3 shows that including the self-energy of the pion changes the in-medium $\bar{K}^*$ width; it becomes, at normal nuclear matter density, about 3 times larger than in vacuum. Including the medium effects of the $\bar{K}$ has a very small effect. The reason that the pion self-energy has such a strong influence lies in the fact that the $\bar{K}^* \to \bar{K}\pi$ decay process leaves the pion with energy right in the region of ΔN^{-1} excitations, where there is considerable pionic strength. When the vertex corrections are included (solid line in Fig. 3), the effect of dressing the pion turns out to be more moderate, giving a $\bar{K}^*$ width of $\Gamma_{\bar{K}^*}(\rho = \rho_0) = 105$ MeV, which is about twice the value of the width in vacuum.

In Fig. 4 the real and imaginary parts of the $\bar{K}^*N \to \bar{K}^*N$ transition amplitude are displayed for different isospin sectors as functions of the center-of-mass energy P_0 for a total momentum $\vec{P} = 0$. We analyze two cases: (i) solution of the on-shell Bethe-Salpeter equation in free space (dashed lines) and (ii) in-medium amplitude at normal nuclear matter density, $\rho_0 = 0.17$ fm^{-3}, including Pauli blocking effects on the nucleon and the $\bar{K}^*$ self-energy in a self-consistent manner (solid lines).

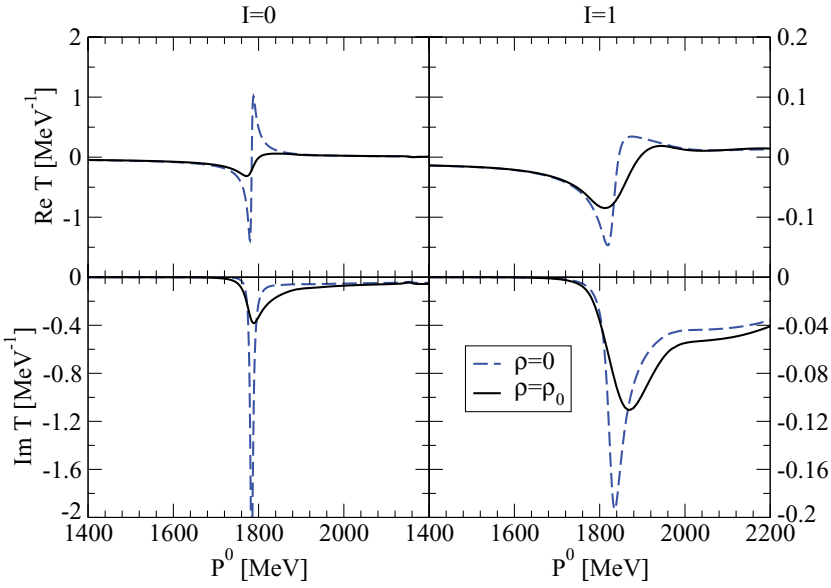

FIG. 4. (Color online) Real and imaginary parts of the $\bar{K}^*N \to \bar{K}^*N$ amplitude as a function of the center-of-mass energy P_0 for a fixed total momentum $|\vec{P}| = 0$. Two new states are generated dynamically: $(I = 0)$ $\Lambda(1783)$ and $(I = 1)$ $\Sigma(1830)$.

From the resonant states that are dynamically generated in free space within the range of energies explored, two of them couple strongly to $\bar{K}^*N$, the $I = 0$ $\Lambda(1783)$ and the $I = 1$ $\Sigma(1830)$ states. They are clearly visible in the corresponding isospin transition amplitude displayed in Fig. 4. As previously discussed in the free-space model developed in Ref. [33], there is one $I = 0$ state in the PDG calculations with $J^P = 1/2^-$, the $\Lambda(1800)$ state, remarkably close to the energy of one of the dynamically generated states. The spin partner is, however, absent in the PDG data or corresponds to the $J^P = 3/2^-$, $\Lambda(1690)$ state, although this would imply a large breaking of the spin degeneracy implicit in the unitary hidden-gauge model. In the $I = 1$ sector, the obtained $\Sigma(1830)$ state was associated with the $J^P = 1/2^-$ PDG state $\Sigma(1750)$ [33]. The widths of both states are, however, smaller than those measured experimentally. We recall that the main source of the imaginary part of the model comes from convoluting the free loop function with the mass distributions for ρ and $\bar{K}^*$ mesons. The inclusion of pseudoscalar baryon decays would make the widths larger and, therefore, closer to the experimental ones.

Medium effects on the transition amplitudes come from two sources. On one hand, we incorporate Pauli blocking on nucleons, an effect that cuts phase space in the unitarized amplitude and pushes the resonances to higher energies. On the other hand, we include the attractive $\bar{K}^*$ self-energy in the $\bar{K}^*N$ intermediate states of the loop function (see later in this section), moving the resonances back to lower energies. As a consequence, the resonances stay close to their free positions. A similar behavior was previously observed for $\Lambda(1405)$ in the pseudoscalar-baryon sector [34,49,63,66,67]. The width of these resonances in matter, however, increases substantially, owing to the opening of new decay channels. Note that the self-consistent $\bar{K}^*N$ effective interaction also incorporates, in the loop function of the intermediate $\bar{K}^*N$ states, the self-energy from the $\bar{K}^* \to \bar{K}\pi$ decay mechanism, shown in Fig. 3. This implements new nucleon absorption possibilities, such as $\bar{K}^*N \to \pi\bar{K}N$ or $\bar{K}^*NN \to \bar{K}NN$.

We show in Fig. 5 the $\bar{K}^*$ self-energy as a function of the $\bar{K}^*$ energy q^0 for zero momentum at normal nuclear matter density. We display the contribution to the self-energy coming from the self-consistent calculation of the $\bar{K}^*N$ effective interaction

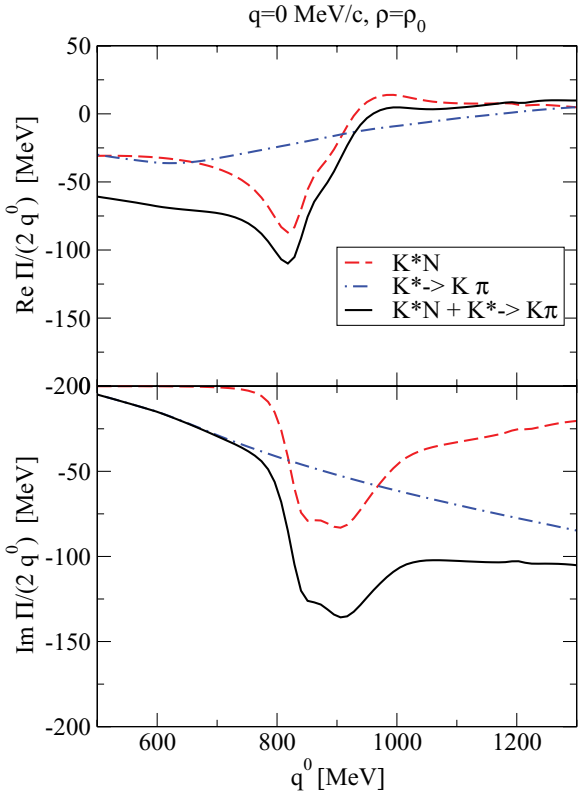

FIG. 5. (Color online) Real and imaginary parts of the $\bar{K}^*$ self-energy as functions of the meson energy q^0 for zero momentum and normal saturation density ρ_0 showing the different contributions: (i) self-consistent calculation of the $\bar{K}^*N$ interaction (dashed lines), (ii) self-energy coming from $\bar{K}^* \to \bar{K}\pi$ decay (dot-dashed lines), and (iii) combined self-energy from both sources (solid lines).

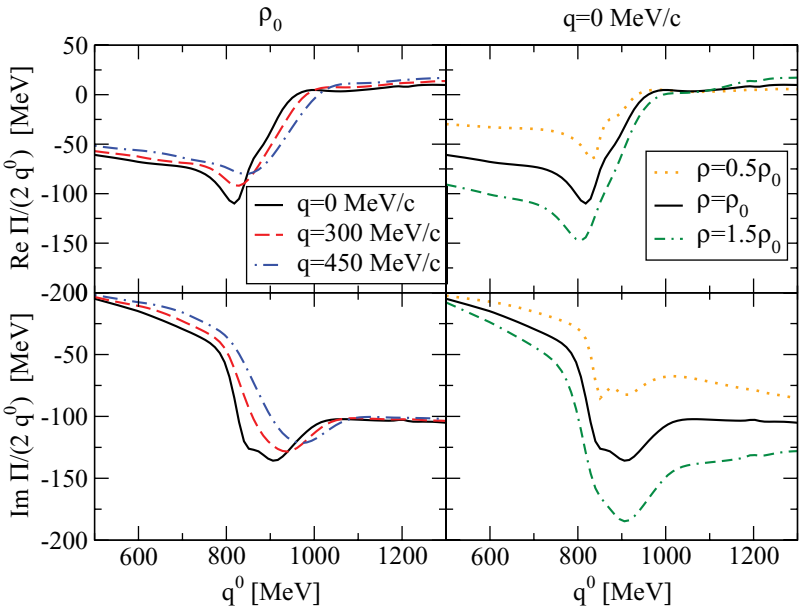

FIG. 6. (Color online) The $\bar{K}^*$ self-energy as a function of the meson energy q^0 for different momenta and densities.

(dashed lines) and the self-energy from the $\bar{K}^* \to \bar{K}\pi$ decay mechanism (dot-dashed lines), together with the combined result from both sources (solid lines).

For $\bar{K}^*$ energies around 800–900 MeV we observe an enhancement of the width together with some structures in the real part of the self-energy. This comes from the coupling of the $\bar{K}^*$ to the dynamically generated $\Lambda(1783)N^{-1}$ and $\Sigma(1830)N^{-1}$ excitations, which dominate the behavior of the $\bar{K}^*$ self-energy in this energy region. However, at lower energies, where the $\bar{K}^*N \to VB$ channels are closed, or as the energy increases, the width of the $\bar{K}^*$ is governed by the $\bar{K}\pi$ decay mechanism in dense matter. At the $\bar{K}^*$ mass, the $\bar{K}^*$ feels a moderately attractive optical potential and acquires a width of 260 MeV, which is about 5 times its width in vacuum.

The behavior of the full $\bar{K}^*$ self-energy with density and momenta is analyzed in Fig. 6, where we display the real and imaginary parts of the self-energy at ρ_0 for different momenta (left panels) and at $q = 0$ MeV/c for different densities (right panels). We observe that the contribution of the resonant-hole states to the self-energy is shifted to higher energies as we move up in momenta, and it increases with density. In general, there is a systematic growth of the imaginary part of the self-energy with the available phase space.

These results are better visualized in the $\bar{K}^*$-meson spectral function, which is displayed in Fig. 7 as a function of the meson energy q^0, for zero momentum and different densities up to $1.5\rho_0$. The dashed line refers to the calculation in free space, where only the $\bar{K}\pi$ decay channel contributes, while the other three lines correspond to fully self-consistent calculations, which also incorporate the process $\bar{K}^* \to \bar{K}\pi$ in the medium.

We observe a rather pronounced peak at the quasiparticle energy

$$\omega_{\rm qp}(\vec{q}=0)^2 = m^2 + {\rm Re}\Pi(\omega_{\rm qp}(\vec{q}=0), \vec{q}=0), \qquad (26)$$

which moves to lower energies with respect to the free $\bar{K}^*$ mass position as the density increases. The $\Lambda(1783)N^{-1}$ and $\Sigma(1830)N^{-1}$ excitations are also clearly visible on the right-hand side of the quasiparticle peak. Despite the fact that the real part of the optical potential, ${\rm Re}\Pi(m_{\bar{K}^*}, \vec{q}=0)/(2m_{\bar{K}^*})$, acquires a moderate value of -50 MeV at ρ_0 (see Fig. 5), interferences with the resonant-hole modes, which appear at energies close to the $\bar{K}^*$ mass, push the quasiparticle peak to a substantially lower energy. Note, however, that the properties of the quasiparticle peak will be affected by the coupling of the $\bar{K}^*$ to other subthreshold excitations, such as $\bar{K}NN^{-1}, \pi YN^{-1}, YN^{-1}, \ldots$, not accounted for in the present model. The peak will be wider, will be less pronounced, and,

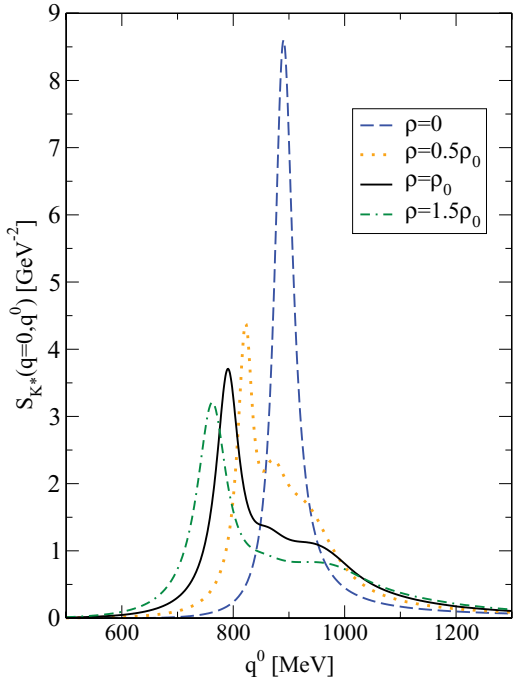

FIG. 7. (Color online) The $\bar{K}^*$ spectral function as a function of the meson energy q^0 for different densities and zero momentum.

through self-consistency, might even be pushed back to higher energies, mixing with the resonant-hole modes, which will also become more extended. Density effects result in a dilution and merging of those resonant-hole states, together with a general broadening of the spectral function owing to the increase in collisional and absorption processes.

From the preceding considerations, a clear conclusion of the present work is that the $\bar{K}^*$ undergoes a tremendous increase in width in matter, a fact that can be tested via a transparency ratio experiment, as discussed in Sec. VI.

V. OVERVIEW OF THE METHOD, CRITICAL DISCUSSION, AND FUTURE DEVELOPMENTS

In this section we comment on the method used, discussing missing terms, with an estimation of their size, as well as other areas where improvements can be made in the future. The first thing that deserves some explanation is why we distinguish between the $\bar{K}^*$ self-energy from the decay into $\bar{K}\pi$ and that coming from the $\bar{K}^*N$ interaction. The main reason is that they provide different sources of inelastic $\bar{K}^*N$ scattering, which sum incoherently in the $\bar{K}^*$ width. Indeed, when studying the s-wave $\bar{K}^*N$ interaction, we have the coupled channels $\bar{K}^*N$, $\omega\Lambda$, $\rho\Sigma$, $\phi\Lambda$, and $K^*\Xi$ for $I = 0$, while for $I = 1$ we consider $\bar{K}^*N$, $\rho\Lambda$, $\rho\Sigma$, $\omega\Sigma$, $K^*\Xi$, and $\phi\Sigma$ (see Sec. II). The inelastic channels are all of the vector meson-baryon type. Instead, for the in-medium corrections to the decay width, represented by the diagram on the right in Fig. 1, we have a pseudoscalar meson and a baryon in the inelastic channels, as the processes induced are of the type $\bar{K}^*N \to \bar{K}N$ when the π excites a ph or the type $\bar{K}^*N \to \pi\Lambda, \pi\Sigma$ when the $\bar{K}$ couples to a Yh excitation. Incidentally, we could have both ph and Yh excitations simultaneously and this would contribute to the absorption channels $\bar{K}^*NN \to \Lambda N, \Sigma N$. All these channels add incoherently to the width of the $\bar{K}^*$, as they correspond to different final states.

Evaluation of the $\bar{K}^*N \to \bar{K}N$ transition amplitude from the diagram in Fig. 1 (right) corresponds to having it mediated by pion exchange, which is a fair assumption. This is different from the way we evaluate the transition amplitudes $\bar{K}^*N \to \bar{K}^*N, VY$ between coupled vector-baryon channels. In this case, we rely on the hidden local gauge approach to derive a tree-level transition potential mediated by vector exchange and use it in a Bethe-Salpeter coupled-channel equation to evaluate the elastic $\bar{K}^*N \to \bar{K}^*N$ amplitude. This amplitude is unitary, and through its imaginary part, via the optical theorem, one makes connection with the vector-baryon inelastic channels. Ideally, one might like to put together the vector-baryon and pseudoscalar-baryon states in the coupled-channel unitary equation. However, at the energies of interest, transitions of the type $\bar{K}^*N \to \bar{K}N$ mediated by pion exchange may allow for this pion to be placed in its mass shell. This forces one to keep track of the proper analytical cuts contributing to the imaginary part of the diagram in Fig. 1 (right), and hence to the $\bar{K}^*$ width, making the iterative problem technically more complicated. Note, also, that because of the VPP and PBB vertices, one is mixing partial waves in the $\bar{K}^*N \to \bar{K}N$ transition. This problem also occurs in other reactions, such as in $\rho\rho \to \rho\rho$, where the ρ can decay into $\pi\pi$, which generates the inelastic channel $\rho\rho \to \pi\pi$ mediated by π exchange (see Refs. [70] and [71]).

A technical solution was provided in the latter works, consisting of calculating the box diagram $\rho\rho \to \pi\pi \to \rho\rho$, with $\rho\rho \to \pi\pi$ mediated by pion exchange, in a field-theoretical way, taking all the cuts into account properly. The resulting $\rho\rho \to \rho\rho$ term was added to the $\rho\rho \to \rho\rho$ potential coming from vector-meson exchange, and the combination was then used as the kernel of the Bethe-Salpeter equation. A welcome feature of this calculation is that the real part of the box diagram is very small and does not change the energies of the dynamically generated resonances. The imaginary part, however, has the effect of inducing an additional width to these resonances, which then stand as largely vector-vector molecules that decay into pseudoscalar-pseudoscalar pairs. The same occurs in the generalization to SU(3) of the vector-vector interaction studied in Ref. [71].

The model of the vector-baryon interaction used here produces quite narrow dynamically generated states compared to the their experimental counterparts, which was precisely attributed in Refs. [32] and [33] to, essentially, the neglect of pseudoscalar-baryon channels. It is clear that including these channels as box diagrams, in complete analogy with what has been done in the vector-vector case, would be most welcome and will be done in the near-future. In the meantime, here we can give an estimation of what the effect of such an improvement would be. We recall, from our discussion of Fig. 7, that the $\bar{K}^*$-induced resonance-hole excitation strength appears as two small bumps in the middle of the wide $\bar{K}^*$ spectral function. Having these resonances with a larger width, from the incorporation of the pseudoscalar-baryon box diagrams, would only lead to a further redistribution of the strength of the spectral function, softening even more the already soft effects of these resonance-hole excitations, without altering our main conclusion about the large width of the $\bar{K}^*$ in nuclei from its many decay channels.

There is another issue worth mentioning. In the approach used in Refs. [32,33,70], and [71], the interaction of vectors with vectors or baryons has been studied at low energies, assuming that the vector three-momenta are small compared to the vector mass. In these circumstances, the approach becomes technically easy, and among other simplifications, one can approximate by a constant the propagator of the vector meson exchanged between the hadronic components. This comes because the momentum transferred $\vec{q}$ is negligible versus the vector meson mass M_V ($\vec{q}^2/M_V^2 \ll 1$), rendering the interaction to be of the contact type. This is implicit in the chiral Lagrangians, which can also be deduced from the hidden gauge approach making this approximation. While this assumption is unquestionable in the limit $\vec{q}^2 \to 0$, there is the fair question of exploring its limits of applicability. This issue is discussed in detail in Sec. 2.2 of Ref. [32], to which we we refer the reader for more details. There, the role of the t-channel exchange of vector mesons, as well as the u-channel processes with baryon exchange, is thoroughly discussed and warnings are given about the danger of misuse when dealing with low-lying energy channels. The conclusion there is that both the local approximation of the t-exchange interaction and the neglect of

u-channel exchange for s waves are well-justified approximations for the range of energies studied in Refs. [32] and [33], which is also the range of relevance in the present work.

A further mechanism when dealing with vector-baryon interaction is the exchange of pseudoscalar mesons rather than vector mesons within the vector-baryon coupled channels. This involves a vector-vector-pseudoscalar vertex, of anomalous type. This mechanism is discussed in Ref. [72], where the $\rho\Delta \to \omega\Delta$ transition was studied in detail. It was shown that the corresponding box diagram, $\rho\Delta \to \omega\Delta \to \rho\Delta$, was negligible compared to the hidden gauge local term of the $\rho\Delta \to \rho\Delta$ interaction. The same conclusion was reached in Ref. [32], where the $\rho\Delta \to \omega N \to \rho\Delta$ box diagram was explicitly evaluated. These findings led to similar conclusions about the contribution of these anomalous terms in the vector-vector interaction [70,71].

Another aspect worth discussing, as it has not been addressed in previous works [32,33,72], concerns the use, in the hidden gauge method, of only the vector-type coupling (γ^μ) of the vector mesons to the baryons, Eq. (6), whereas the tensor-type coupling ($\sigma^{\mu\nu}$), known to be sizable for the ρNN case, is neglected. The ρNN coupling reads [73]

$$-\mathrm{i}t_{\rho NN} = \mathrm{i}\left(G^V\gamma^\mu + \frac{G^T}{2\mathrm{i}M_N}\,\sigma^{\mu\nu}\,q_\nu\right)\epsilon^*_\mu\tau^a, \qquad (27)$$

with $G^V = 2.9 \pm 0.3$ and $G^T = 18 \pm 2$, where q_μ is the ρ momentum and ϵ_μ is its polarization vector. The nonrelativistic reduction of this vertex reads [73]

$$-\mathrm{i}t_{\rho NN} = \mathrm{i}\left(G^E\epsilon^0 - \frac{G^M}{2M_N}\,(\vec{\sigma}\times\vec{q})\vec{\epsilon}\right)\tau^a, \qquad (28)$$

with $G^E = G^V$ and $G^M = G^V + G^T$.

This tensor coupling in the case of the ρ is known to be relevant when studying the nucleon-nucleon tensor force and the spin-isospin excitation modes in nuclei [74]. Yet, for the case of the vector-baryon interaction, the situation is quite different. Indeed, as shown in Refs. [32] and [33], the three-vector vertex, VVV, in Fig. 8(b) is the same as the PPV in Fig. 8(a) for small values of the three-momentum of the vector mesons. The problem of neglecting the tensor-type coupling in the lower VBB vertex is therefore also present in the study of the interaction of pseudoscalar mesons with baryons. Yet this interaction has traditionally been tackled by means of chiral Lagrangians [75,76], which stem from the diagram in Fig. 8(a), calculated within the hidden gauge approach, neglecting $\vec{q}^2/M_V^2$ and considering only the γ^μ

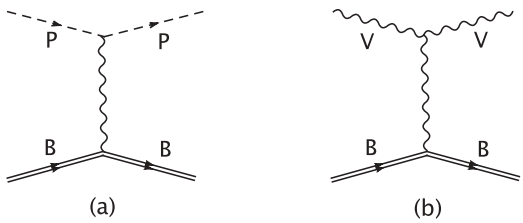

FIG. 8. Diagrams of contributions to (a) the pseudoscalar-baryon or (b) the vector-baryon interaction via exchange of a vector meson.

coupling of the VBB vertex. The success of the chiral unitary approach in the meson-baryon interaction suggests that there must be a good justification to neglect the tensor coupling in this type of problems. Because this has not been explicitly exposed in earlier work, we take the opportunity here to make estimates of the relevance of this term. Indeed, let us consider the transition $K^{*-}p \to K^{*-}p$, represented by the diagram in Fig. 8(b). For small three-momenta of the vector mesons, the VVV vertex behaves as the PPV vertex in the diagram in Fig. 8(a), namely, $(k+k')_\mu\epsilon^\mu$, with k, k' the momenta of the kaons and ϵ^μ the vector polarization. When contracting this vertex with the BBV one in Eq. (28), we get two contributions,

$$G^E(k^0 + k'^0), \quad G^M\left(\frac{\vec{\sigma}\times\vec{q}}{2M_N}\right)(\vec{k}+\vec{k}'), \qquad (29)$$

with $\vec{q} = \vec{k} - \vec{k}'$, by means of which we obtain, close to the $K^{*-}p$ threshold, the terms $2G^E M_V$ versus $\frac{G^M}{M_N}\vec{\sigma}(\vec{k}\times\vec{k}')$.

First, note that these two terms belong to different partial waves and they do not add coherently. The term with G^M also vanishes when we evaluate the $t\rho$ optical potential in nuclear matter for the $\bar{K}^*$, where t stands for the forward $K^{*-}p \to K^{*-}p$ amplitude. The contribution of the magnetic term to the $\bar{K}^*$ potential, or to the imaginary part of the $\bar{K}^*N \to \bar{K}^*N$ amplitude, comes from the angled averaged amplitude squared, $\int d\Omega|T|^2$. We also recall that the $K^{*-}K^{*-}\rho$ and $K^{*-}K^{*-}\omega$ vertices are the same and that the γ^μ part of the ωpp vertex is three times larger than the corresponding one of the ρpp vertex, while the tensor ωpp one is negligible. Taking all these considerations into account and assuming $|\vec{k}| = |\vec{k}'| \approx 300$ MeV, when evaluating $\mathrm{Im}t_{\bar{K}^*p\to\bar{K}^*p}$, or the cross section, the relative contribution of the magnetic ρ term to the sum of the ρ and ω electric terms turns out to be of the order of 0.7% (2% for $|\vec{k}| = |\vec{k}'| \approx 500$ MeV). This exercise justifies *a posteriori* why the magnetic ρNN coupling has been systematically neglected in chiral dynamics studies of the meson-baryon or vector-baryon interaction and, for our purposes, why we neglect it here too.

VI. NUCLEAR TRANSPARENCY IN THE $\gamma A \to K^+K^{*-}A'$ REACTION

In this section we make a qualitative evaluation of the nuclear transparency ratio by comparing the cross sections of the photoproduction reaction $\gamma A \to K^+K^{*-}A'$ in different nuclei and tracing them to the in-medium width of the K^{*-}. The idea is that the survival probability is an exponential function of the integral of the in-medium width and, hence, very sensitive to this magnitude [29].

We write the nuclear transparency ratio as

$$\tilde{T}_A = \frac{\sigma_{\gamma A\to K^+K^{*-}A'}}{A\sigma_{\gamma N\to K^+K^{*-}N}}, \qquad (30)$$

that is, the ratio of the nuclear K^{*-}-photoproduction cross section divided by A times the same quantity for a free nucleon. The value of $\tilde{T}_A$ describes the loss of flux of K^{*-} mesons in the nucleus and is related to the absorptive part of the K^{*-}-nucleus optical potential and thus to the K^{*-} width in

the nuclear medium. This method has already been proven to be very efficient in the study of the in-medium properties of vector mesons [25,77,78], hyperons [79], and antiprotons [29]. In Refs. [30] and [80] the transparency ratio was used to determine the width of the ω meson in finite nuclei using a BUU transport approach.

We have done calculations for a vast sample of nuclear targets: ${}^{12}_{6}$C, ${}^{14}_{7}$N, ${}^{23}_{11}$Na, ${}^{27}_{13}$Al, ${}^{28}_{14}$Si, ${}^{35}_{17}$Cl, ${}^{32}_{16}$S, ${}^{40}_{18}$Ar, ${}^{50}_{24}$Cr, ${}^{56}_{26}$Fe, ${}^{65}_{29}$Cu, ${}^{89}_{39}$Y, ${}^{110}_{48}$Cd, ${}^{152}_{62}$Sm, ${}^{207}_{82}$Pb, and ${}^{238}_{92}$U. In the following, we evaluate the ratio between the nuclear cross sections in heavy nuclei and a light nucleus, for instance, ^{12}C, as, in this way, many other nuclear effects not related to absorption of the K^{*-} cancel in the ratio [77]. We call this ratio T_A,

$$T_A = \frac{\tilde{T}_A}{\tilde{T}_{^{12}C}}, \tag{31}$$

and by construction, it is normalized to unity for ^{12}C.

We obtain the nuclear transparency ratio taking an eikonal (or Glauber) approximation in the evaluation of the distortion factor associated with K^{*-} absorption. In this framework, the propagation of the K^{*-} meson on its way out of the nucleus is implemented by means of the exponential factor for the survival probability accounting for the loss of flux per unit length. This simple but rather reliable method allows us to get an accurate result for the integrated cross sections.

We proceed as follows: let $\Pi_{K^{*-}}$ be the K^{*-} self-energy in the nuclear medium as a function of the nuclear density $\rho(r)$. We then have

$$\frac{\Gamma_{K^{*-}}}{2} = -\frac{\mathrm{Im}\Pi_{K^{*-}}}{2E_{K^{*-}}}, \quad \Gamma_{K^{*-}} \equiv \frac{dP}{dt}, \tag{32}$$

where P is the probability of K^{*-} interactions in the nucleus, including K^{*-} quasielastic collisions and absorption channels. There is some problem when dealing with the free part of the K^{*-} self-energy. Indeed, if the K^{*-} decays inside the nucleus into $\bar{K}\pi$, the $\bar{K}$ or the π will also be absorbed with a high probability or undergo a quasielastic collision, such that the $\bar{K}\pi$ invariant mass will no longer be that of the K^{*-}. Thus, it is adequate to remove these events. Yet if the decay occurs at the surface, neither the $\bar{K}$ nor the π will be absorbed and an experimentalist will reconstruct the K^{*-} invariant mass from these two particles, in which case they should not be removed from the flux. The part of $\mathrm{Im}\Pi_{K^{*-}}$ owing to quasielastic collisions $K^{*-}N \to K^{*-}N$ should not be taken into account in the distortion either, as the K^{*-} does not disappear from the flux in these processes. Yet this part is small at low energies and we disregard this detail in the present qualitative estimate. In view of all this, we have taken the following approximate choice for $\mathrm{Im}\Pi_{K^{*-}}$ in our estimate of T_A:

$$\mathrm{Im}\Pi_{\bar{K}^*} = \begin{cases} (-2.5\times10^5 + 0.4\times10^5)\rho(r)/\rho_0\ \mathrm{MeV}^2 - 0.4\times10^5\ \mathrm{MeV}^2 & \text{for} \quad r < 0.8R, \\ (-2.5\times10^5 + 0.4\times10^5)\rho(r)/\rho_0\ \mathrm{MeV}^2 & \text{for} \quad r \geqslant 0.8R, \end{cases} \tag{33}$$

where R is the nuclear radius. The choice of Eq. (33) is justified by the fact that $\mathrm{Im}\Pi_{\bar{K}^*} = -2.5\times10^5$ MeV^2 at $q^0 = m_{\bar{K}^*}$ and $\vec{q} = 0$ MeV/c at $\rho = \rho_0$ (see Fig. 6). This value also contains the contribution from the free decay, $\mathrm{Im}\Pi^0_{\bar{K}^*} \simeq -0.4\times10^5$ MeV^2, which does not depend on ρ. It therefore needs to be subtracted from the term that implements the linear ρ dependence and added as a constant value if $r < 0.8R$. Moreover, when the $\bar{K}^* \to \bar{K}\pi$ decay takes place on the surface of the nucleus, $r \geqslant 0.8R$, we remove $\mathrm{Im}\Pi^0_{\bar{K}^*}$, as experimentally the $\bar{K}\pi$ system will be reconstructed as a $\bar{K}^*$.

The probability of loss of flux per unit length is given by

$$\frac{dP}{dl} = \frac{dP}{vdt} = \frac{dP}{\frac{|\vec{p}_{K^{*-}}|}{E_{K^{*-}}}dt} = -\frac{\mathrm{Im}\Pi_{K^{*-}}}{|\vec{p}_{K^{*-}}|}, \tag{34}$$

and the corresponding survival probability is determined from

$$\exp\left\{\int_0^\infty dl \frac{\mathrm{Im}\Pi_{K^{*-}}(\rho(\vec{r}\,'))}{|\vec{p}_{K^{*-}}|}\right\}, \tag{35}$$

where $\vec{r}\,' = \vec{r} + l\frac{\vec{p}_{K^{*-}}}{|\vec{p}_{K^{*-}}|}$, with $\vec{r}$ being the K^{*-} production point inside the nucleus.

With all these ingredients and taking into account the standard expression for K^{*-} production in the nucleus prior to consideration of the eikonal distortion, the cross section for the $\gamma A \to K^+K^{*-}A'$ reaction is obtained from

$$\begin{aligned} \sigma_{\gamma A\to K^+K^{*-}A'} = {} & \frac{M^2}{4(s-M^2)}\frac{1}{(2\pi)^4}\int d^3r\rho(r) \\ & \times \int_{m_{K^{*-}}}^{E_2^{\max}} p_2\, dE_2 \int_{m_{K^+}}^{E_3^{\max}} dE_3 \int_{-1}^{1} d\cos\theta_2 \\ & \times \int_0^{2\pi} d\phi_2 \frac{1}{|\vec{p}_\gamma - \vec{p}_2|} \\ & \times \theta(1-A^2)\theta(E_\gamma + M - E_2 - E_3)|T|^2 \\ & \times \exp\left\{\int_0^{2.5R} dl\, \mathrm{Im}\Pi(\rho(\vec{r}\,'))/p_2\right\}, \end{aligned} \tag{36}$$

with

$$\begin{aligned} A \equiv \cos\theta_3 = {} & \frac{1}{2|\vec{p}_\gamma - \vec{p}_2|p_3}\left\{M^2 + |\vec{p}_\gamma - \vec{p}_2|^2 + \vec{p}_3^{\,2}\right. \\ & \left. - (E_\gamma + M - E_2 - E_3)^2\right\} \end{aligned} \tag{37}$$

and

$$\begin{aligned} E_2^{\max} &= \frac{s + m_{K^{*-}}^2 - (M + m_{K^+})^2}{2\sqrt{s}}, \\ E_3^{\max} &= \frac{s + m_{K^+}^2 - (M + m_{K^{*-}})^2}{2\sqrt{s}}, \end{aligned} \tag{38}$$

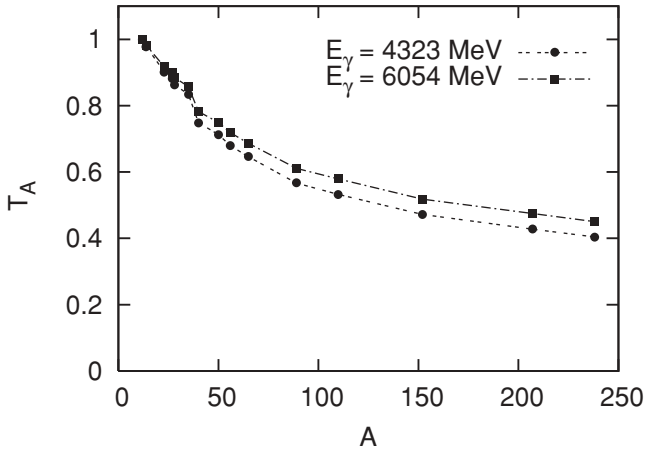

FIG. 9. Transparency ratio.

where $(E_2, \vec{p}_2)$ and $(E_3, \vec{p}_3)$ are the four-momenta of the K^{*-} and K^+, respectively, in the frame of the nucleon at rest, and E_γ is the energy of the photon in this frame. Here, M is the mass of the nucleon, while $m_{K^{*-}}$ and m_{K^+} are the masses of the K^{*-} and K^+ mesons, respectively. The value of $E_2^{\max}$ has been calculated when particles 1 plus 3 go together (or particles 1 plus 2 in the case of $E_3^{\max}$). Because we are interested in the ratios of cross sections, we have taken $|T|^2 = 1$.

The results are shown in Fig. 9, where the transparency ratio is plotted for two energies in the center-of-mass reference system $\sqrt{s} = 3$ and 3.5 GeV, which are equivalent to the energies of the photon in the laboratory frame, 4.3 and 6 GeV, respectively. We observe a very strong attenuation of the $\bar{K}^*$ production process owing to the decay or absorption channels $\bar{K}^* \to \bar{K}\pi$ and $\bar{K}^* N \to YY$ with increasing nuclear-mass number A. This is caused by the larger path that the $\bar{K}^*$ has to follow before it leaves the nucleus, thus having more chances to decay or get absorbed.

VII. CONCLUSIONS

We have studied the properties of $\bar{K}^*$ mesons in symmetric nuclear matter within a self-consistent coupled-channel unitary approach using hidden gauge local symmetry. The corresponding in-medium solution incorporates Pauli blocking effects and the $\bar{K}^*$ meson self-energy in a self-consistent manner. In particular, we have analyzed the behavior of dynamically generated baryonic resonances in the nuclear medium and their influence on the self-energy and, hence, the spectral function of $\bar{K}^*$ mesons.

We have found a moderate attractive optical potential for the $\bar{K}^*$, of the order of -50 MeV, at normal nuclear matter density. The corresponding quasiparticle peak in the spectral function might not be easily distinguished, owing to its merging with other excitations, apart from the fact that changes in mass are always very difficult to determine in experiments [28]. More remarkable are the changes in width, which can be addressed more easily by means of transparency ratios in different reactions. At normal nuclear matter density the $\bar{K}^*$ width is found to be about 260 MeV, 5 times larger than its free width. This spectacular increase is much larger than the width of the ρ meson in matter, evaluated theoretically in Refs. [6–9] or measured recently [12,14,17,18].

We have estimated the transparency ratios in the $\gamma A \to K^+ \bar{K}^* A'$ reaction and found a substantial reduction from unity in the magnitude, which should be easier to observe experimentally. Other reactions such as $K^- A \to K^{*-} A'$ should also be good tools for investigating these important changes linked to the strong $\bar{K}^*$ interaction with the nuclear medium [81].

ACKNOWLEDGMENTS

L.T. wishes to acknowledge support from the Rosalind Franklin Programme of the University of Groningen (The Netherlands) and the Helmholtz International Center for FAIR within the framework of the LOEWE program of the State of Hesse (Germany). This work was partly supported by Project Nos. FIS2006-03438 and FIS2008-01661 of the Ministerio de Ciencia e Innovación (Spain) and by the Generalitat Valenciana within the program Prometeo and by Generalitat de Catalunya Contract No. 2009SGR-1289. This research is part of the European Community-Research Infrastructure Integrating Activity "Study of Strongly Interacting Matter" (HadronPhysics2; Grant No. 227431) and of the EU Human Resources and Mobility Activity FLAVIAnet (Contract No. MRTN–CT–2006–035482) under the EU Seventh Framework Programme.

[1] R. Rapp and J. Wambach, Adv. Nucl. Phys. **25**, 1 (2000).
[2] R. S. Hayano and T. Hatsuda, Rev. Mod. Phys., arXiv:0812.1702 [nucl-ex].
[3] S. Leupold, V. Metag, and U. Mosel, Int. J. Mod. Phys. E **19**, 147 (2010).
[4] V. Bernard and U. G. Meissner, Nucl. Phys. A **489**, 647 (1988).
[5] G. E. Brown and M. Rho, Phys. Rev. Lett. **66**, 2720 (1991).
[6] R. Rapp, G. Chanfray, and J. Wambach, Nucl. Phys. A **617**, 472 (1997).
[7] W. Peters, M. Post, H. Lenske, S. Leupold, and U. Mosel, Nucl. Phys. A **632**, 109 (1998).
[8] M. Urban, M. Buballa, and J. Wambach, Nucl. Phys. A **673**, 357 (2000).
[9] D. Cabrera, E. Oset and M. J. Vicente Vacas, Nucl. Phys. A **705**, 90 (2002).
[10] M. Post, S. Leupold, and U. Mosel, Nucl. Phys. A **741**, 81 (2004).
[11] D. Cabrera and M. J. Vicente Vacas, Phys. Rev. C **67**, 045203 (2003).
[12] R. Arnaldi *et al.* (NA60 Collaboration), Phys. Rev. Lett. **96**, 162302 (2006).
[13] S. Damjanovic *et al.* (NA60 Collaboration), Nucl. Phys. A **783**, 327 (2007).
[14] R. Arnaldi *et al.* (NA60 Collaboration), Eur. Phys. J. C **59**, 607 (2009).
[15] H. van Hees and R. Rapp, Nucl. Phys. A **806**, 339 (2008).

[16] R. Rapp and J. Wambach, Eur. Phys. J. A **6**, 415 (1999).
[17] M. H. Wood *et al.* (CLAS Collaboration), Phys. Rev. C **78**, 015201 (2008).
[18] C. Djalali, M. H. Wood, R. Nasseripour, and D. P. Weygand (CLAS Collaboration), J. Phys. G **35**, 104035 (2008).
[19] R. Muto *et al.* (KEK-PS-E325 Collaboration), Phys. Rev. Lett. **98**, 042501 (2007).
[20] M. Naruki *et al.*, Phys. Rev. Lett. **96**, 092301 (2006).
[21] J. C. Caillon and J. Labarsouque, J. Phys. G **21**, 905 (1995).
[22] K. Saito, K. Tsushima, D. H. Lu, and A. W. Thomas, Phys. Rev. C **59**, 1203 (1999).
[23] M. F. M. Lutz, G. Wolf, and B. Friman, Nucl. Phys. A **706**, 431 (2002); **765**, 495(E) (2006).
[24] P. Muehlich, V. Shklyar, S. Leupold, U. Mosel, and M. Post, Nucl. Phys. A **780**, 187 (2006).
[25] M. Kaskulov, E. Hernandez, and E. Oset, Eur. Phys. J. A **31**, 245 (2007).
[26] M. Kaskulov, H. Nagahiro, S. Hirenzaki, and E. Oset, Phys. Rev. C **75**, 064616 (2007).
[27] D. Trnka *et al.* (CBELSA/TAPS Collaboration), Phys. Rev. Lett. **94**, 192303 (2005).
[28] M. Nanova *et al.* (TAPS Collaboration), Phys. Rev. C **82**, 035209 (2010).
[29] E. Hernandez and E. Oset, Z. Phys. A **341**, 201 (1992).
[30] M. Kotulla *et al.* (CBELSA/TAPS Collaboration), Phys. Rev. Lett. **100**, 192302 (2008).
[31] C. Garcia-Recio, J. Nieves, and L. L. Salcedo, Phys. Rev. D **74**, 034025 (2006).
[32] S. Sarkar, B. X. Sun, E. Oset, and M. J. V. Vacas, Eur. Phys. J. A **44**, 431 (2010).
[33] E. Oset and A. Ramos, Eur. Phys. J. A **44**, 445 (2010).
[34] A. Ramos and E. Oset, Nucl. Phys. A **671**, 481 (2000).
[35] E. Oset and A. Ramos, Nucl. Phys. A **635**, 99 (1998).
[36] M. Bando, T. Kugo, S. Uehara, K. Yamawaki, and T. Yanagida, Phys. Rev. Lett. **54**, 1215 (1985).
[37] M. Bando, T. Kugo, and K. Yamawaki, Phys. Rep. **164**, 217 (1988).
[38] M. Harada and K. Yamawaki, Phys. Rep. **381**, 1 (2003).
[39] U. G. Meissner, Phys. Rep. **161**, 213 (1988).
[40] H. Nagahiro, L. Roca, A. Hosaka, and E. Oset, Phys. Rev. D **79**, 014015 (2009).
[41] Riazuddin and Fayyazuddin, Phys. Rev. **147**, 1071 (1966).
[42] J. J. Sakurai, *Currents and Mesons* (The University of Chicago Press, Chicago, IL, 1969).
[43] F. Klingl, N. Kaiser, and W. Weise, Nucl. Phys. A **624**, 527 (1997).
[44] J. E. Palomar and E. Oset, Nucl. Phys. A **716**, 169 (2003).
[45] J. A. Oller and U. G. Meissner, Phys. Lett. B **500**, 263 (2001).
[46] L. Roca, E. Oset, and J. Singh, Phys. Rev. D **72**, 014002 (2005).
[47] C. Amsler *et al.* (Particle Data Group), Phys. Lett. B **667**, 1 (2008).
[48] H. Nagahiro, L. Roca, and E. Oset, Eur. Phys. J. A **36**, 73 (2008).
[49] L. Tolos, A. Ramos, and E. Oset, Phys. Rev. C **74**, 015203 (2006).
[50] E. Oset, P. Fernandez de Cordoba, L. L. Salcedo, and R. Brockmann, Phys. Rep. **188**, 79 (1990).
[51] A. Ramos, E. Oset, and L. L. Salcedo, Phys. Rev. C **50**, 2314 (1994).
[52] T. Waas, N. Kaiser, and W. Weise, Phys. Lett. B **379**, 34 (1996).
[53] T. Waas and W. Weise, Nucl. Phys. A **625**, 287 (1997).
[54] C. Garcia-Recio, J. Nieves, T. Inoue, and E. Oset, Phys. Lett. B **550**, 47 (2002).
[55] E. Oset and A. Ramos, Nucl. Phys. A **679**, 616 (2001).
[56] G. Q. Li, C. H. Lee, and G. E. Brown, Nucl. Phys. A **625**, 372 (1997).
[57] G. Q. Li, C. H. Lee, and G. E. Brown, Phys. Rev. Lett. **79**, 5214 (1997).
[58] L. Tolos, C. Garcia-Recio, and J. Nieves, Phys. Rev. C **80**, 065202 (2009).
[59] G. Mao, P. Papazoglou, S. Hofmann, S. Schramm, H. Stöcker, and W. Greiner, Phys. Rev. C **59**, 3381 (1999).
[60] J. Schaffner and I. N. Mishustin, Phys. Rev. C **53**, 1416 (1996).
[61] J. Schaffner, J. Bondorf, and I. N. Mishustin, Nucl. Phys. A **625**, 325 (1997).
[62] K. Tsushima, K. Saito, A. W. Thomas, and S. V. Wright, Phys. Lett. B **429**, 239 (1998); **436**, 453(E) (1998).
[63] M. Lutz, Phys. Lett. B **426**, 12 (1998).
[64] J. Schaffner-Bielich, V. Koch, and M. Effenberger, Nucl. Phys. A **669**, 153 (2000).
[65] A. Cieply, E. Friedman, A. Gal, and J. Mares, Nucl. Phys. A **696**, 173 (2001).
[66] L. Tolos, A. Ramos, A. Polls, and T. T. S. Kuo, Nucl. Phys. A **690**, 547 (2001).
[67] L. Tolos, A. Ramos, and A. Polls, Phys. Rev. C **65**, 054907 (2002).
[68] M. Herrmann, B. L. Friman, and W. Norenberg, Nucl. Phys. A **560**, 411 (1993).
[69] G. Chanfray and P. Schuck, Nucl. Phys. A **555**, 329 (1993).
[70] R. Molina, D. Nicmorus, and E. Oset, Phys. Rev. D **78**, 114018 (2008).
[71] L. S. Geng and E. Oset, Phys. Rev. D **79**, 074009 (2009).
[72] P. Gonzalez, E. Oset, and J. Vijande, Phys. Rev. C **79**, 025209 (2009).
[73] D. Jido, E. Oset, and J. E. Palomar, Nucl. Phys. A **709**, 345 (2002).
[74] E. Oset, H. Toki, and W. Weise, Phys. Rep. **83**, 281 (1982).
[75] G. Ecker, Prog. Part. Nucl. Phys. **35**, 1 (1995).
[76] V. Bernard, N. Kaiser, and U. G. Meissner, Int. J. Mod. Phys. E **4**, 193 (1995).
[77] V. K. Magas, L. Roca, and E. Oset, Phys. Rev. C **71**, 065202 (2005).
[78] P. Muhlich and U. Mosel, Nucl. Phys. A **765**, 188 (2006).
[79] M. M. Kaskulov and E. Oset, Eur. Phys. J. A **28**, 139 (2006); M. Kaskulov, L. Roca, and E. Oset, Phys. Rev. C **73**, 045213 (2006).
[80] P. Muhlich and U. Mosel, Nucl. Phys. A **773**, 156 (2006).
[81] C. Djalali (private communication).